Acoustic shielding in a fan stage predicted with two fast analytical models

Antoine Moreau[1]

[1] DLR, Institute of Propulsion Technology, Engine Acoustics Department, Germany, Email: antoine.moreau@dlr.de

I. Introduction

A major source responsible for fan noise is the interaction of the front rotor with the stator, or outlet guide vanes (OGV). Due to the presence of the nacelle, the sound generated between rotor and OGV is forced to propagate upstream through the rotor and downstream through the OGV before exiting the engine and radiating into the far field. It is known that the acoustic shielding produced by the rotor is very substantial, especially when the tip speed operates at supersonic conditions. The present paper proposes to quantify this shielding effect by applying two simple analytical models to a realistic transonic fan test case and comparing their predictions with the experimentally measured sound power emitted by the fan stage.

II. Propagation angles of acoustic modes

Acoustic modes propagating inside a duct can be described by their propagation phase and group propagation angles ζ and ξ, respectively. In general the phase and group velocity vectors are computed as follows:

$$\begin{cases} \mathbf{c}_\zeta = c_0 \left(1 + \mathbf{M} \cdot \mathbf{n}_\zeta\right) \mathbf{n}_\zeta \\ \mathbf{c}_\xi = c_0 \left(\mathbf{M} + \mathbf{n}_\zeta\right) \end{cases} \tag{1}$$

With the two-dimensional assumption, the flow velocity vector and the unit wavefront vector are given by:

$$\begin{cases} \mathbf{M} = M_x \mathbf{e}_x + M_\theta \mathbf{e}_\theta \\ \mathbf{n}_\zeta = \cos\zeta \mathbf{e}_x - \sin\zeta \mathbf{e}_\theta \end{cases} \tag{2}$$

Moreover, the dispersion relation can be written as follows, where $\tilde{k}$ is the apparent wavenumber and $k = 2\pi f / c_0$ is the wavenumber in a medium at rest:

$$\begin{cases} \tilde{k} = \sqrt{k_x^2 + k_\theta^2} = k - k_\theta M_\theta - k_x M_x \\ \text{thus: } k_x = \left(k - k_\theta M_\theta\right) \frac{-M_x \pm \alpha}{1 - M_x^2} \\ \text{with } \alpha = \sqrt{1 - \left(1 - M_x^2\right) \frac{k_\theta^2}{\left(k - k_\theta M_\theta\right)^2}} \text{(cut-on param.)} \\ \text{and } k_\theta = \frac{m}{r} \text{(2}\pi\text{-periodicity)} \end{cases} \tag{3}$$

The parameter m is the circumferential mode order and assumes only integer values, and r is the radius of the radial strip at which the propagation is considered. Finally combining the previous equations (1,2,3) together, we obtain the phase propagation angle ζ:

$$\cos\zeta = \frac{k_x}{\tilde{k}} = \frac{-M_x \pm \alpha}{1 \mp \alpha M_x} \tag{4}$$

This expression is valid for cut-on modes only, for cut-off modes the imaginery part of α should be ignored. It should be also noted that ζ, unlike ξ, is an invariant if considered in the absolute or in the relative rotor frame, which means it remains unchanged when changing the frame of reference. Figure 1 shows schematically the two-dimensional model of the problem and the related geometric parameters. Note that with a rotating blade row, the flow Mach vector $\mathbf{M}_{rel}$ is modified to account for the rotation movement of the rotor.

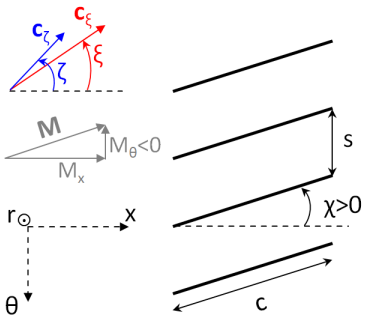

Figure 1: Simplified modeling of sound transmission through a fixed blade row.

The flow is assumed to be parallel with the blades in the relative frame, which corresponds to the zero-incidence assumption. Moreover, the flow is assumed uniform across the blade row and the representative values are taken at the leading edge, as they are the more restrictive ones for the transmission (higher Mach number and larger stagger angle, for a compressor-type blade).

III. Analytical transmission models with a 2D approach

In the present chapter two analytical models for the prediction of sound transmission through a blade row are described and discussed. Both models are asymptotic approximations for low and high frequencies. Both models are fundamentally two-dimensional with blade row modeled as flat plates in the presence of flow under zero incidence. Only the transmission coefficient is calculated and the sound scattering and reflection mechanisms are ignored.

a) Amiet's low-frequency model

Amiet [1] was one of the few researchers to derive a closed-form, thus very simple, analytical model for the transmission through a 2D blade row with flow; however it has a low-frequency restriction. The main parameters of Amiet's model are the phase propagation angle ζ, the flow Mach number in the relative frame of the blade row M_{rel}, the blade solidity σ (defined as the chord-to-pitch

ratio) and the blade stagger angle χ. The transmission factor of the sound pressure amplitude is given by the following expressions:

$$\begin{cases} \text{upstream: } T = 1 - \frac{M_{rel}\cdot\sin^2(\zeta-\chi)}{M_{rel}\cdot\sin^2(\zeta-\chi)+\mathcal{L}\cdot(M_x+\cos\zeta)} \\ \text{downstream: } T = 1 - \frac{M_{rel}\cdot\sin^2(\zeta-\chi)}{M_{rel}\cdot X+\mathcal{L}\cdot(M_x+\cos\zeta)} \\ \text{where } X = \frac{\left(\sin(\zeta-\chi)+\frac{2(M_x+\cos\zeta)}{1-M_x^2}\sin\chi\right)^2}{1+\frac{2M_x(M_x+\cos\zeta)}{1-M_x^2}} \end{cases} \quad (5)$$

where $\mathcal{L} = \mathcal{L}(\sigma, \chi, M_{rel})$ is the Lattice parameter is a function of the solidity, the stagger angle and the relative Mach number. Note that Amiet's model predicts full sound transmission if the relative flow Mach number vanishes, irrespective of the blade geometry.

b) Ray-based geometric model

The second model to be tested corresponds to the high-frequency approximation, where the sound propagation can be represented by rectilinear rays, propagating along the group velocity angle ξ_{rel} in the relative reference frame. The rays bounce on the blade surfaces and are transmitted with a reduced intensity through the blade row. The sound power transmission coefficient is calculated based on the number of bounces N and on some empirical energy damping coefficient after each bounce τ, which is here introduced by the author:

$$\begin{cases} T = \tau^N, \text{ where } N = \frac{\sigma}{\cos\chi}\cdot\tan\phi \\ \text{with } \tan\phi = \frac{\mathbf{c}_\xi\cdot\mathbf{e}_n}{\mathbf{c}_\xi\cdot\mathbf{e}_\ell} = \frac{\sin(\zeta-\chi)}{M_{rel}+\cos(\zeta-\chi)} \\ \text{or } \tan\phi = 1/\tan(\xi_{rel}-\chi+\pi/2) \end{cases} \quad (6)$$

It should be mentioned that the parameter τ is not directly physical, because the blade surfaces are hard walls. This has to be regarded as an empirical coefficient, whose value is chosen at $\tau = 0.9$ for the present study.

c) Validation of the models

Both low- and high-frequency models are now applied to a cascade transmitting sound in the downstream direction and compared in Fig. 2 with the more complex analytical model by Smith (1972) and a numerical CAA method called 'LIN3D', this test case is detailed in Behn et al [2]. The simple models capture the main properties of sound transmission: the full transmission of modes whose phase angle is aligned with the blades, the asymmetric transmission of positive- and negative-order modes, and the poor transmission of near-cutoff modes.

The next figure illustrates the behavior of the models when the flow Mach number is varied from 0.1 to 0.9. For the upstream propagation, the range of well transmitted modes narrows continuously as sonic conditions become closer. It should be noted that in the case of very low Mach number, Amiet's model almost predicts full transmission whereas the geometric model predicts more shielding. For the downstream case, the range of transmission narrows similarly in Amiet's model, but on the contrary it becomes broader in the geometric model.

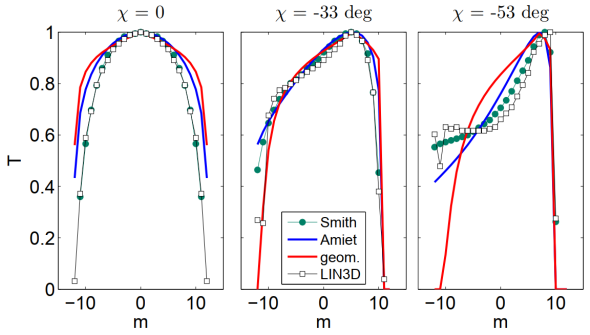

Figure 2: Validation of the transmission models on a 2D cascade with $M_{rel} \approx 0.2$.

However we will see in the next chapter than downstream shielding is very small, so accurate predictions there are far less important than for the upstream shielding.

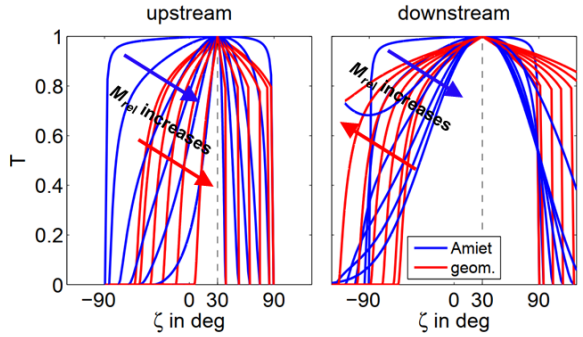

Figure 3: Effect of Mach number on the transmission through a 2D cascade with $\chi = 30°$.

IV. Application to a realistic fan stage

The analytical models discussed in the previous section are fundamentally two-dimensional. It is possible to extend their application to a realistic three-dimensional fan test case by applying a strip approach, where several sections of the rotor and stator are considered for the transmission of sound on a 2D basis. In this chapter, the sound power generated by the interaction of the rotor wakes with the OGV (only its broadband component) and transmitted through the stage will be calculated for various speed regimes based on the present analytical approach, and also a semi-empirical correlation approach by NASA; the results are compared with test data.

a) Presentation of the test case

The fan stage considered here for application of the shielding models is the ACAT1 fan, which was extensively tested within the EU-funded project *TurboNoiseBB*. It has a fan pressure ratio around 1.4 near its design point, with a rotor relative tip Mach number of 1.14. The simplified model used for the analytical prediction is shown in Fig. 4, only the bypass through the OGV is modelled and the core flow through the inlet guide vanes (IGV) is ignored; but the main geometric parameters of the fan stage are respected (blade count, chord, stagger angles and axial distance).

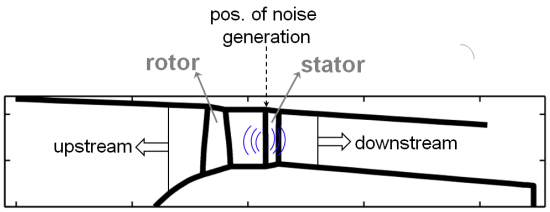

Figure 4: Side view of the simplified ACAT1 fan stage model.

Acoustic predictions require an estimation of the aerodynamic performance, which is performed by the mean-line aerodynamic model of PropNoise [3]. The estimated aerodynamic performance map of the ACAT1 fan is shown in Fig. 5. The stage pressure ratio is plotted against the non-dimensional mass flow Q/Q_{max} along iso-speed lines depicted in gray, and along the high-loading and low-loading working lines in black and blue, respectively.

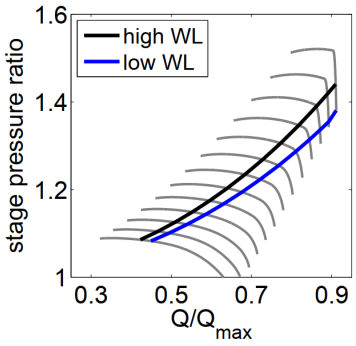

Figure 5: Estimated aerodynamic performance map of the ACAT1 fan stage with iso-speed lines (in gray) and the two considered working lines.

b) Comparison of OAPWL

In this paragraph, the evolution of the overall sound power of the broadband rotor-stator interaction noise source is predicted for various rotation speeds along two working lines. The analytical models first estimate the sound power generated at the source (near the OGV leading edge) [3] and then calculates the shielding by the rotor for the upstream-propagating sound, and the shielding of the downstream-propagating sound through the OGV. The analytical predictions are compared with a NASA semi-empirical correlation by Kontos [4] and with experimental data in Fig. 6.

Note that the experimental upstream sound power is obtained from far-field microphones located in the forward arc (with a correction that removes the atmospheric damping), whereas the downstream sound power is estimated based on the wavenumber decomposition of sound pressure levels measured with in-duct wall-flush mounted microphones and with a modal energy distribution model [5].

For the upstream radiation (left part of the figure), the increase of OAPWL up to a relative tip Mach number

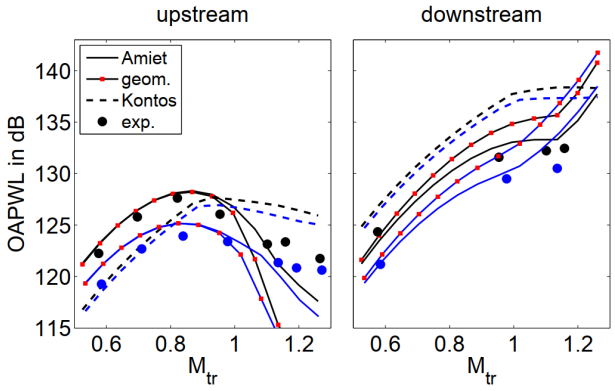

Figure 6: Evolution of radiated sound power (left: upstream, right: downstream) along the high working line (black color) and low working line (blue color).

$M_{tr} = 0.85$ is very well predicted by the analytical approach, for both working lines, and for both transmission models (Amiet's and geometric model). Beyond this point, the stronger shielding by the rotor compensates the increase in noise generation and the transmitted OAPWL decreases toward high values of M_{tr}. The slope in the test data is however less pronounced than what the models predict; this may be attributable to the presence of other noise sources at the rotor or at the IGV, which are close to the hub and are thus weakly shielded by the rotor (less staggered blades and lower Mach number).

For the downstream radiation (right part of the figure), a continuous increase in OAPWL is observed along the working lines. The slope becomes lower as the tip speed is increased because the rotor blades operate under less aerodynamic incidence as the design point is reached ($M_{tr} = 1.14$ on the black curve), thus producing smaller wakes and less turbulence impacting the downstream OGV. The rapid increase in OAPWL predicted by the analytical model beyond the design point is caused by the choking of the fan rotor, which abruptly modifies the rotor exit flow conditions and may be overestimated when compared to the test data.

c) Comparison of sound power transmission

Now the focus is put on the magnitude of the shielding itself. Fig. 7 shows on the left part the so-called 'transmission loss' across rotor (upstream) and the OGV (downstream), which is the ratio of incoming sound power to transmitted sound power through the corresponding blade row. Both Amiet's and the geometric models predict very similar trends: a much higher shielding caused by the rotor, which rapidly increases with the tip speed. The shielding by the OGV is relatively weak and increases slowly with tip speed. The geometric model predicts a stronger rotor shielding than Amiet's model, but a weaker shielding by the OGV.

On the right part of Fig. 7, the difference between downstream and upstream propagated sound power is compared with NASA's correlation and the test data. At

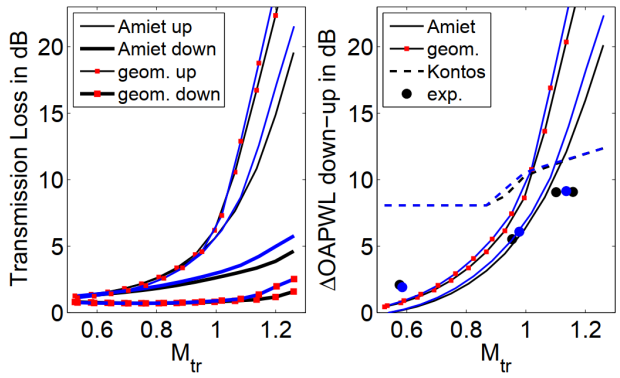

Figure 7: Transmission loss across rotor and stator (left), and sound power difference between downstream and upstream radiated noise (right), shown along the high and low working lines (black and blue colors, resp.).

subsonic tip speeds, the analytical models match better with the experiments than the semi-empirical correlation by Kontos. At supersonic speeds, as already mentioned, the model overprediction is attributed to the presence of other broadband sources capable to radiate in the upstream direction, such as sources on the rotor or the IGV.

d) Comparison of sound pressure spectra

So far only the sound power integrated over all frequencies and modes has been considered. Here a closer look is taken at the behavior predicted by the models in the frequency domain. Fig. 8 depicts the spectra of the downstream-upstream sound power difference for the operating conditions Approach ($M_{tr} = 0.58$), Cut-Back ($M_{tr} = 0.93$), and the Aerodynamic Design Point / Cruise ($M_{tr} = 1.14$). As the quantities of interest here are more refined than a global OAPWL value, larger discrepancies are observed locally between measurements and predictions. In particular, the slight bump of ΔPWL at mid-frequencies is not captured at all by the models. However, the average slope of ΔPWL from low to high frequencies and its drift from Approach to Cruise seems to be roughly captured, which is encouraging provided both transmission models do not include the frequency as a parameter due to their asymptotic nature (low- and high-frequency approximations).

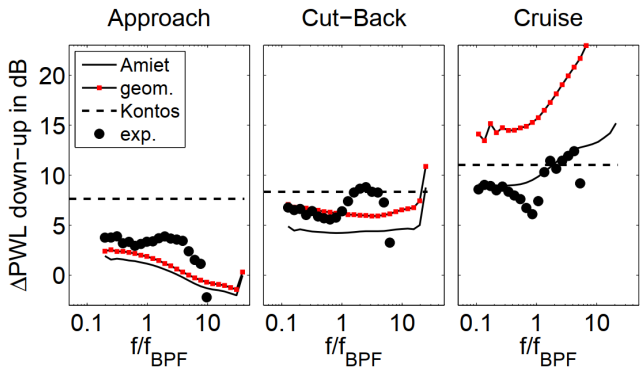

Figure 8: Spectra of sound power difference between downstream and upstream transmitted noise for three operating points.

V. Conclusion

The present study has shown that simple analytical models are able to estimate well the acoustic shielding of the rotor-stator wake interaction, one of the dominant fan broadband noise sources in modern civil-aircraft engines. As a result, the prediction of sound power transmitted upstream of the rotor and downstream of the OGV is significantly improved, especially in the high-speed operating regime.

Despite the strongly simplifying 2D flat-plate strip approach, both low-frequency and high-frequency models properly capture the main effects of the shielding mechanism, which are the flow Mach number and stagger angle of the rotor blades.

Possible model refinement may account for real-blade geometry, varying flow conditions at the blade-row leading and trailing edges, sound scattering and reflection, or the presence of weakly shielded sound generated by the inlet guide vanes of the core engine. However, the accuracy increase to be expected from these more complex models is likely to be marginal for the purpose of preliminary design. Future work will rather focus on extending the validation test cases to the tonal component of the rotor-stator interaction, and to other fan stages.

Acknowledgments

This work was funded by the German Federal Ministry for Economic Affairs and Energy, as part of the LuFo V research project *MAMUT* (grant number 20T1524C). The author also thanks Dr. Sébastien Guérin and the consortium of the EU-funded project *TurboNoiseBB* (grant number 690714) for sharing and processing the ACAT1 fan test data.

References

[1] R. Amiet. Transmission and reflection of sound by a blade row. AIAA 9th Aerospace Sciences Meeting, New York, USA, AIAA 71-181, 1971.

[2] M. Behn et al. Comparative study of different analytical approaches for modelling the transmission of sound waves through turbomachinery stators. 22nd AIAA/CEAS Aeroacoustics Conference, Lyon, France, AIAA 2016-2927, 2016.

[3] A. Moreau. A unified analytical approach for the acoustic conceptual design of fans of modern aeroengines. PhD thesis, Technical University of Berlin, 2017.

[4] K. Kontos et al. Improved NASA-ANOPP noise prediction computer code for advanced subsonic propulsion systems, vol.1. NASA Contractor Report 195480, 1996.

[5] U. Tapken et al. Radial mode breakdown of the ACAT1 fan broadband noise generation in the bypass duct using a sparse sensor array. 25th AIAA/CEAS Aeroacoustics Conference, Delft, The Netherlands, AIAA 2019-2525, 2019.